Chemistry of Metals and Alloys

Chem. Met. Alloys 11 (2018) 92-99
Ivan Franko National University of Lviv
www.chemetal-journal.org

On the binary phases ~YNi_4 and Y_2Ni_7

Volodymyr BABIZHETSKYY[1]*, Oksana MYAKUSH[2], Volodymyr LEVYTSKYI[1], Bogdan KOTUR[1], Viola DUPPEL[3], Lorentz KIENLE[4]

[1] *Department of Inorganic Chemistry, Ivan Franko National University of Lviv, Kyryla i Mefodiya St. 6, UA-79005 Lviv, Ukraine*
[2] *National University of Forest and Wood Technology of Ukraine, Chuprynky St. 103, UA-79057 Lviv, Ukraine*
[3] *Max Planck Institute for Solid State Research, Heisenbergstr. 1, Postfach 800665, D-70569 Stuttgart, Germany*
[4] *Institute for Material Science, Christian Albrechts University Kiel, Kaiserstr. 2, D-24143 Kiel, Germany*
* *Corresponding author. E-mail: v.babizhetskyy@googlemail.com*

Received October 1, 2018; accepted December 26, 2018; available on-line March 29, 2019

Y–Ni alloys in the composition range 79-81 at.% Ni, annealed at 600°C and 800°C, were investigated by complementary analytical techniques providing chemical and structural information. In contradiction to former reports, the ~YNi_4 phase was not observed at these temperatures. The samples annealed at 600°C consisted of two phases: the rhombohedral HT β-Y_2Ni_7 phase (structure type β-Gd_2Co_7, space group *R*-3*m*) and YNi_5 (structure type $CaCu_5$, space group *P6/mmm*). At 800°C the hexagonal LT form α-Y_2Ni_7 (structure type Ce_2Ni_7 type, space group *P*6$_3$/*mmc*) was found to coexist with HT β-Y_2Ni_7. The transformation β-Y_2Ni_7 ↔ α-Y_2Ni_7 is very sluggish and increasing the annealing time to five months increased the amount of α-Y_2Ni_7 only up to ~23%. The transformation β-Y_2Ni_7 ↔ α-Y_2Ni_7 occurs at *T* > 800°C, but a more precise determination was not possible. The ~YNi_4 phase exists in a very narrow temperature range: it forms by the peritectic reaction $YNi_5 + L$ ↔ ~YNi_4 at 1338±2°C and decomposes by the metatectic reaction ~YNi_4 ↔ $L + YNi_5$ at 1328±2°C. The section YNi_5–Y_2Ni_7 of the phase diagram of the binary Y−Ni system was revised consequently.

Intermetallics / Phase diagram / Crystal structure / X-ray diffraction

Introduction

The Y–Ni phase diagram was first investigated by Beaudry and Daane [1] and later by Domagala *et al.* [2]. Both groups agree on the occurrence of the following binary compounds: Y_3Ni, Y_3Ni_2, YNi, YNi_2, YNi_3, YNi_4, and YNi_5, however, the conclusions differ concerning the composition of the Ni-richest compound, which is defined as YNi_9 [2] and Y_2Ni_{17} [1], respectively. Later, Buschow [3] confirmed the data of [1], and the composition Y_2Ni_{17} was also accepted in several other reports [4-6]. An additional difference between the two early investigations is that Beaudry and Daane [1] report an additional phase Y_2Ni_7 between YNi_4 and YNi_3, whereas Domagala *et al.* [2] do not. Neither of these investigations provides information about the structures of the compounds YNi_4 and Y_2Ni_7. Later [7,8], two types of structure were reported for Y_2Ni_7: a hexagonal structure of Ce_2Ni_7 type (space group *P*6$_3$/*mmc*) [9] and a rhombohedral structure of β-Gd_2Co_7 type (space group *R*-3*m*) [10]. It is not clear from the data reported in the literature, which of these structures is actually adopted by a given modification of Y_2Ni_7. The authors of [8,11] conclude that the hexagonal form is stable at low temperatures (600°C [8] and 500-850°C [11]) whereas the rhombohedral modification is the high-temperature (> 1100°C [8]) modification of Y_2Ni_7. However, other scientists [12-14] suggest that the hexagonal form is stable at high temperatures (> 1100°C), the rhombohedral form being the low-temperature (< 950°C) modification. This contradiction may stem from the fact that the two structure types are closely related, since both are derivatives of the hexagonal $CaCu_5$ type [11,12,15]. Attempts to obtain single-phase samples containing one of the two modifications of Y_2Ni_7 were unsuccessful [7-10,12-20]. The authors of [7-10,12-20] did not study the detailed crystal structures of the Y_2Ni_7 modifications, but refined the lattice parameters. Buschow and van der Goot [12] suggested that the transformation between the two forms is of the martensitic type and that the crystal structure of the R_2Ni_7 (*R* = rare earth) compounds depends on the size of the rare-earth element. They conclude that, because of the small difference in stability between the hexagonal and rhombohedral modifications, it is likely that the occurrence of one or

the other modification strongly depends on the conditions of synthesis.

Beaudry and Daane [1] investigated the conditions and temperature of formation of the YNi_4 compound and observed that their $Y_{19.9}Ni_{80.1}$ alloy was single phase only after annealing at 1250°C. The crystal structure of YNi_4 was not established, because the intensities in the X-ray powder patterns were quite diffuse in the low-angle region and faded out completely at high scattering angles. The authors explained the diffuse X-ray pattern by a large contraction of the unit cell in one direction upon cooling, resulting in strain and non-periodic distortion of the lattice. The EDX and XRD analyses of a sample of composition $Y_{18.8}Ni_{81.2}$, annealed at a lower temperature (1150°C), indicated the presence of two phases: YNi_5 ($CaCu_5$-type structure) and YNi_4 (unknown structure). Based on these data, Beaudry and Daane [1] concluded that the compound YNi_4 is stable from room temperature up to 1340°C. However, the existence of the YNi_4 phase is questionable, since it was not observed in other studies [12,13]. The authors of [4-6,16-19] confirmed the existence of YNi_4, but did not report its crystal structure. Moreover, in [19] the formation of an extended solid solution based on the binaries YNi_4 and YCu_4 with unknown structure was reported. Later, a systematic study of the phase equilibria in the Y–Ni–Cu [14] and Y–Zr–Ni ternary systems at 600°C [20] did not confirm the existence of YNi_4. Metallographic and XRD analysis of an $Y_{20}Ni_{80}$ (≡YNi_4) sample annealed at 600°C showed the presence of two phases with compositions $Y_{18(1)}Ni_{82(1)}$ and $Y_{22(1)}Ni_{78(1)}$, respectively [20]. The $Y_{18(1)}Ni_{82(1)}$ phase was refined as hexagonal YNi_5 ($CaCu_5$-type structure, *P6/mmm*), while the crystal structure of the second phase $Y_{22(1)}Ni_{78(1)}$ remained unknown.

In this study we present a reinvestigation of three alloys in the composition range 79-81% Ni by means of X-ray diffraction (XRD), high-resolution transmission electron microscopy (HRTEM) and electron diffraction, with the aim to clarify the conditions of formation and existence of ~YNi_4. Another aim was to study the occurrence of the Y_2Ni_7 modifications and their dependence on the preparation conditions.

Experimental procedure

Three alloys of composition $Y_{19}Ni_{81}$, $Y_{20}Ni_{80}$, and $Y_{21}Ni_{79}$ were prepared by arc-melting elements with a purity not less than 99.9 wt.% under argon. During arc melting the weight losses were below 1% of the total mass of the ingots. The alloys were annealed in evacuated quartz ampoules at 600°C for one month, and at 800°C for five months, and quenched in cold water.

The phase analysis of the alloys was carried out using X-ray diffraction (XRD) data obtained with a DRON-2.0 (Fe *K*α radiation) or a STOE STADI P (Mo $K\alpha_1$) diffractometer. X-ray powder diffraction patterns for full-profile refinements were collected on the powder diffractometer STOE STADI P with monochromated Cu $K\alpha_1$ radiation ($20 \le 2\theta \le 120°$, step size 0.1°, scan time 200 s). For the profile refinement the CSD program package [21] was used.

Metallographic, and quantitative and qualitative composition analyses of polished samples were performed by energy-dispersive X-ray (EDX) spectroscopy on a scanning electron microscope TESCAN 5130MM equipped with an Oxford Si-detector and an Oxford WAVE 700 detector. The samples were ground and dispersed in *n*-butanol.

One drop of suspension was transferred to a holey carbon / copper grid for high-resolution transmission electron microscopy (HRTEM). The electron microscopy experiments were carried out with a Philips CM 30ST microscope (LaB_6 cathode, 300 kV, C_S = 1.15 mm). Selected area electron diffraction in precession mode (PED) was performed using a diaphragm that limited the diffraction to a circular area of 250 nm in diameter. Chemical analyses by EDX were performed with a Si/Li detector (Noran, Vantage System). Quantitative EDX results were based on the average of five measurements each.

High-temperature differential thermal analysis (DTA) was carried out under argon atmosphere (Linseis STA PT 1600). A ceramic crucible containing 48.5(5) mg of the $Y_{20}Ni_{80}$ sample was heated to 1360°C and cooled to room temperature at a constant heating and cooling rate of 10°C/min in one cycle. The thermal effects of the phase transitions, obtained from the DTA curves, were evaluated using the device software with an accuracy of ±1°C.

Results and discussion

The full-profile analysis of the XRD pattern of the $Y_{20}Ni_{80}$ sample annealed at 600°C (see Fig. 1) and the EDX analysis (see Fig. 2d) indicated the presence of two phases: $Y_{18(1)}Ni_{82(1)}$ (YNi_5) ($CaCu_5$-type structure) and $Y_{22(1)}Ni_{78(1)}$ (Y_2Ni_7) (rhombohedral β-Gd_2Co_7-type structure). The hexagonal form of Y_2Ni_7 was not observed. Crystallographic data for both phases in the $Y_{20}Ni_{80}$ sample are presented in Table 1. Atomic coordinates and displacement parameters are given in Table 2.

The lattice parameters of YNi_5 ($CaCu_5$-type structure) are in good agreement with the literature data [1,4,11]. However, the lattice parameters of rhombohedral Y_2Ni_7 are significantly larger than those reported in [7,8,12,13] (see Table 1). According to [8] the cell parameters of Y_2Ni_7 (β-Gd_2Co_7-type structure) are a = 4.924, c = 36.07 Å. The difference (~2% in cell volume) may be explained by different conditions of synthesis, annealing temperature and time, which may have resulted in deviations from the ideal 2:7 composition, as previously observed for off-stoichiometric $Dy_{2-x}Ni_7$ [22,23].

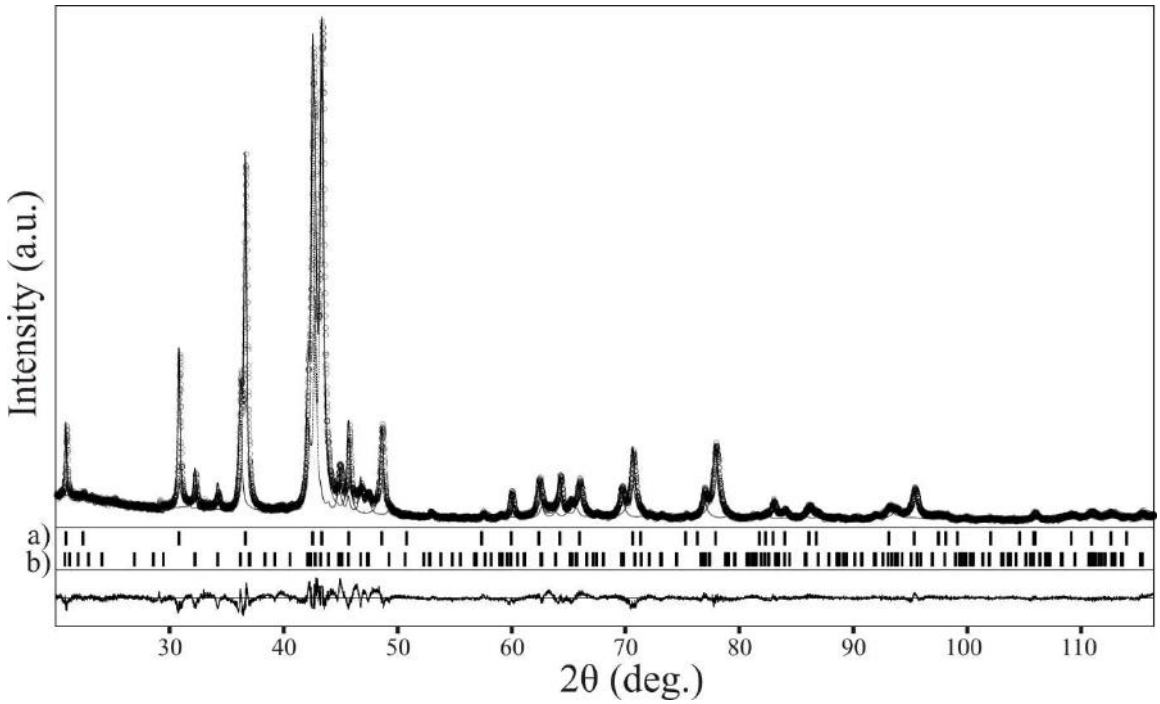

Fig. 1 XRD profile of the $Y_{20}Ni_{80}$ alloy annealed at 600°C (calculated profile (line), observed profile (dots), difference (bottom)). Vertical bars indicate the reflections from the $Y_{18(1)}Ni_{82(1)}$ phase ($CaCu_5$-type structure) (a) and the $Y_{22(1)}Ni_{78(1)}$ phase (β-Gd_2Co_7-type structure) (b). Thin lines show the calculated contribution of both compounds to the total experimental XRD profile.

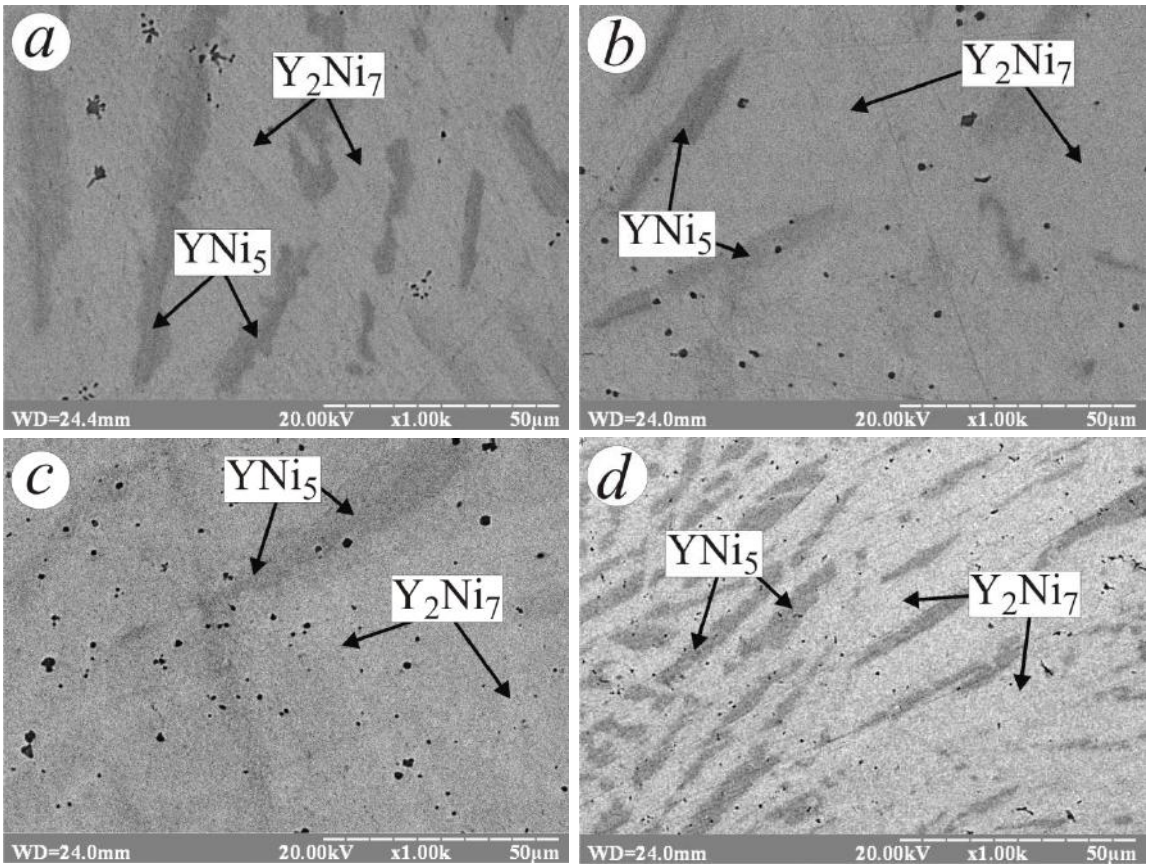

Fig. 2 Microstructure of the $Y_{19}Ni_{81}$ (a), $Y_{20}Ni_{80}$ (b), and $Y_{21}Ni_{79}$ (c) samples annealed at 800°C, and of the $Y_{20}Ni_{80}$ (d) sample annealed at 600°C; dark phase – $Y_{18(1)}Ni_{82(1)}$, light phase – $Y_{22(1)}Ni_{78(1)}$.

Table 1 Refinement details and crystallographic data for the phases in the $Y_{20}Ni_{80}$ alloy annealed at 600°C.

	Phase 1	Phase 2
Empirical formula	$Y_{18(1)}Ni_{82(1)}$	$Y_{22(1)}Ni_{78(1)}$
Phase content (%)	76.36	23.64
Structure type	$CaCu_5$	β-Gd_2Co_7
Space group	*P6/mmm*	*R*-3*m*
Lattice parameters: *a* (Å)	4.8966(1)	4.9525(3)
c (Å)	3.9605(2)	36.314(3)
Unit cell volume (Å^3)	82.239(7)	771.4(2)
F(000) (electrons)	179.0	1644.0
Number of atoms in the unit cell	6.0	54.0
Calculated density (g/cm^3)	7.7218(7)	7.604(2)
Absorption coefficient (1/cm)	511.39	550.31
Radiation and wavelength (Å)	Cu *Kα*$_1$, 1.54056	
Diffractometer	STOE STADI P (powder)	
Mode of refinement	Full profile	
Number of atom sites	3	7
Two-theta and sin*θ*/*λ*, max (°, 1/Å)	117.0, 0.553	142.0, 0.614
R_I, R_p	0.085, 0.146	0.104, 0.146
Scale factor	0.02298	0.39065
Texture axis and parameter	[0 0 1], 4.04(3)	[0 0 1], 2.06(4)

Table 2 Atomic coordinates and isotropic displacement parameters (Å^2) for the phases in the $Y_{20}Ni_{80}$ alloy annealed at 600°C.

Phase 1, *P6/mmm*						Phase 2, *R*-3*m*					
Atom	Site	*x*	*y*	*z*	B_{iso}	Atom	Site	*x*	*y*	*z*	B_{iso}
Y1	1*a*	0	0	0	0.74(4)	Y1	6*c*	0	0	0.0487(3)	0.9(2)
Ni1	2*c*	⅓	⅔	0	0.38(5)	Y2	6*c*	0	0	0.1523(2)	0.47(12)
Ni2	3*g*	½	0	½	0.23(4)	Ni1	3*b*	0	0	½	0.5(1) [a]
						Ni2	6*c*	0	0	0.2820(3)	0.5(1)
						Ni3	6*c*	0	0	0.3842(3)	0.5(1)
						Ni4	9*e*	½	0	0	0.5(1)
						Ni5	18*h*	0.5018(8)	-*x*	0.1123(2)	0.5(1)

[a] restrained to be identical for all Ni sites

In order to corroborate the absence of the hexagonal form of Y_2Ni_7 in the $Y_{20}Ni_{80}$ sample homogenized at 600°C, we studied this alloy also by PED. The PED patterns of the $Y_{20}Ni_{80}$ alloy, taken along the fundamental directions of the hexagonal system ([001], [100], and [210] for different crystallites), are presented in Fig. 3. The quasi-kinematic intensity in the PED patterns (right hand-side) is well reproduced by simulations based on the kinematic theory (left hand-side) assuming $CaCu_5$-type structure (*P6/mmm*). Similar agreement was observed for crystallites assigned to the two polymorphs of the Y_2Ni_7 structure (β-form: rhombohedral *R*, α-form: hexagonal *P*), see Fig. 4a,b. However, diffuse streaks along *c** were frequently observed in the electron diffraction patterns and Fourier transforms of the HRTEM micrographs as an additional feature. The HRTEM micrographs (Fig. 4c), together with contrast simulations (insets in Fig. 4c), prove that planar defects such as intergrowth of single YNi_5-type layers (not shown), and stacking variants according to an aperiodic mixture of α- and β-type stacking, cause the diffuse streaks, The letter code in Fig. 4c indicates the different positions of consecutive layers (β-type: ABC, α-type: AC).

The fact that the hexagonal α-Y_2Ni_7 form was detected by PED in the sample $Y_{20}Ni_{80}$ annealed at 600°C, but not identified by EDX or XRD analysis, can only indicate that the content of this phase is very small. It can be assumed that with increasing temperature and time of annealing, the content of α-Y_2Ni_7 phase will increase.

The obtained data indicate that the ~YNi_4 phase does not exist at 600°C or 800°C, but it may exist at higher temperatures. To verify this assumption the $Y_{20}Ni_{80}$ sample was studied by DTA in the temperature range 20-1360°C. A fragment of the high-temperature part of the DTA curve of the $Y_{20}Ni_{80}$ sample is shown in Fig. 5.

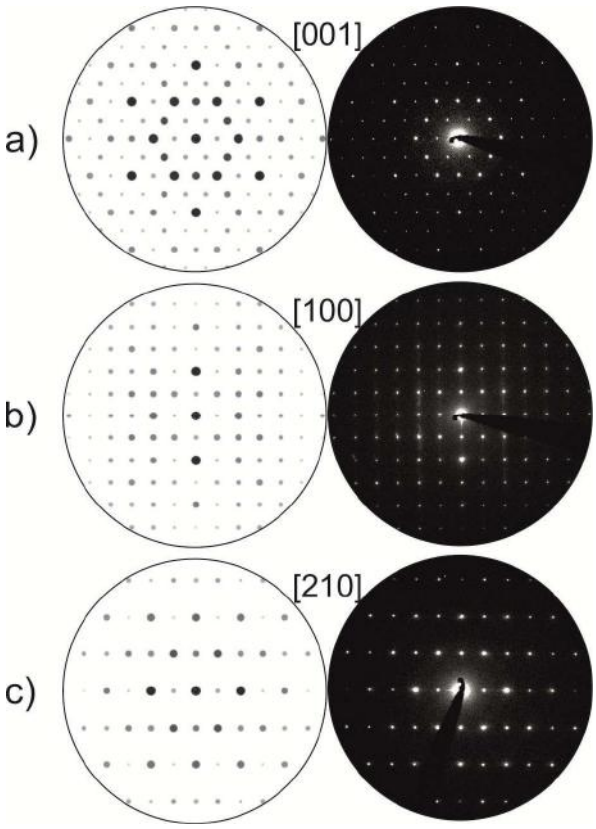

Fig. 3 Right hand-side: PED patterns recorded along the fundamental zone axes of single crystalline areas of the YNi_5 phase in the $Y_{20}Ni_{80}$ sample annealed at 600°C; left hand-side: simulated patterns based on the kinematic theory: [001] (a), [100] (b), [210] (c).

The temperatures of the invariant transformations $YNi_5 + L \leftrightarrow$ ~YNi_4 and ~$YNi_4 \leftrightarrow YNi_5 + L$, deduced from the curve (summarized in Table 3), are in good agreement with the literature data [1,2,4-6]. The DTA analysis showed that the ~YNi_4 phase only exists in a very narrow temperature range from 1338±2°C to 1328±2°C. Due to the limited working domain of the DTA device, higher temperatures could not be reached.

In order to compare the results of the present work with literature data on the relative stability of the Y_2Ni_7 modifications [4-13,15-19], we increased the annealing temperature and time. Diffuse broadening in the XRD profiles of the $Y_{19}Ni_{81}$, $Y_{20}Ni_{80}$, and $Y_{21}Ni_{79}$ alloys annealed at 800°C for 5 months (see Fig. 6), is clearly seen in the angular region from 36 to 48° 2θ. The broadening corresponds to the transformation of the rhombohedral into the hexagonal form of Y_2Ni_7 and the coexistence of both modifications. EDX (Fig. 2a-c) and XRD (Fig. 6) analyses of the alloys annealed at 800°C confirmed that the three samples have similar XRD patterns and consist of the YNi_5 phase ($CaCu_5$-type structure) and mixtures of the two forms of Y_2Ni_7, with different ratios of YNi_5 and Y_2Ni_7. The observed microstructures proved the coexistence of the two forms within one crystallite. In agreement with literature data [8,13], we conclude that rhombohedral β-Y_2Ni_7 is the high-temperature modification, formed by the peritectic reaction $YNi_5 + L \leftrightarrow$ β-Y_2Ni_7. We found that short-term annealing of an as-cast sample at 600°C was insufficient to cause complete β-Y_2Ni_7 to α-Y_2Ni_7 transformation. When the temperature was raised to 800°C and the annealing time increased to five months, partial transformation of rhombohedral β-Y_2Ni_7 to the hexagonal α-Y_2Ni_7 form, with a yield of ~23% (Fig. 6), was observed.

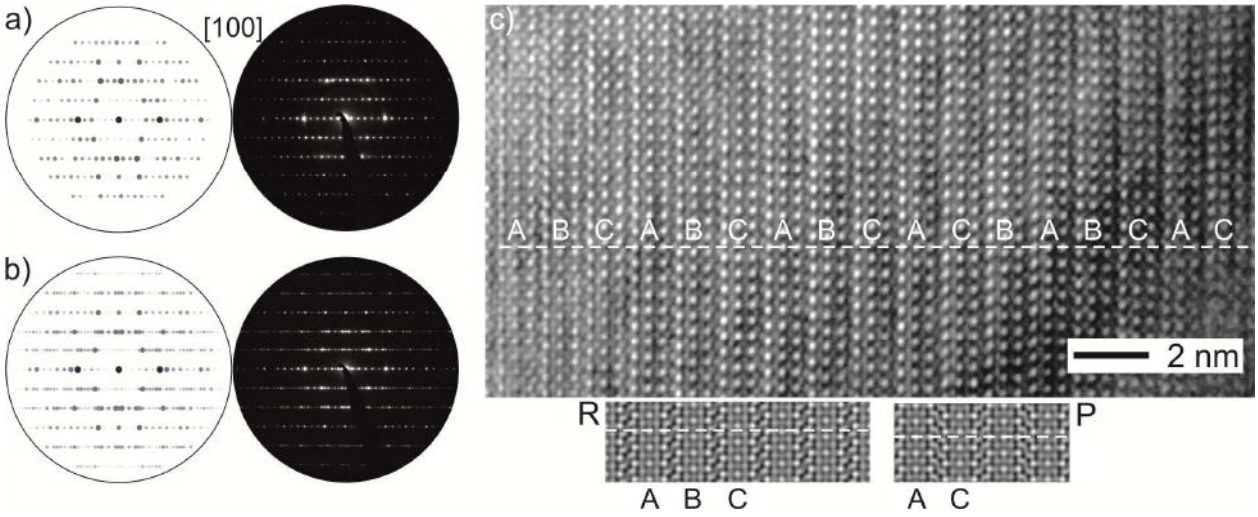

Fig. 4 a) and b) PED [100] zone axis patterns recorded on single crystalline areas of Y_2Ni_7 in the $Y_{20}Ni_{80}$ sample annealed at 600°C: β-form (rhombohedral *R*) (a), α-form (hexagonal *P*) (b). Left hand-side: simulated patterns (kinematic theory), right hand-side: experimental PED patterns. c) HRTEM micrograph with inserted multislice contrast simulations (crystal thickness: 2.96 nm, defocus value: -80 nm) based on the structures of the β-form (ABC) and α-form (AC), respectively (see text).

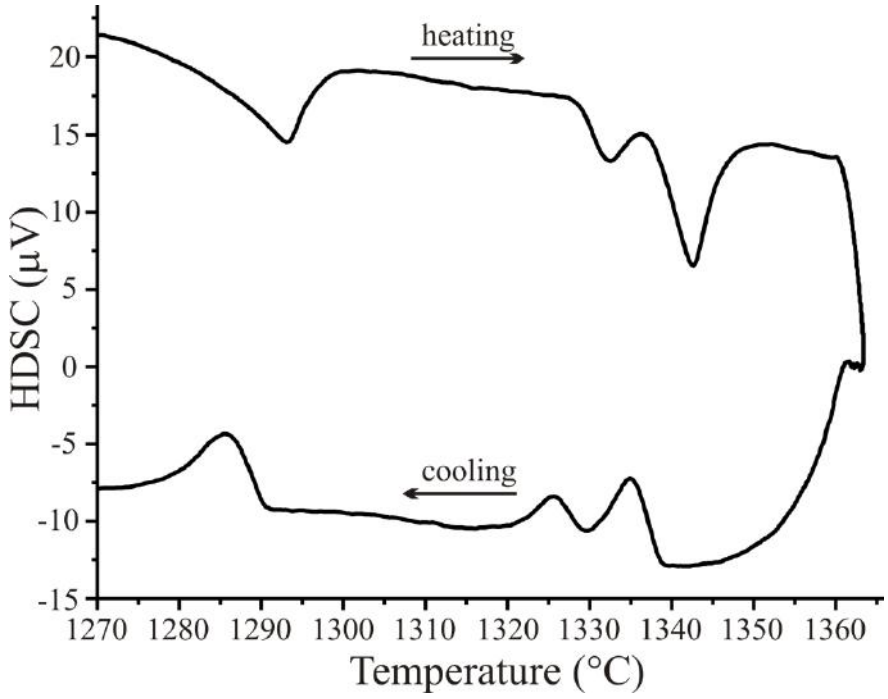

Fig. 5 High-temperature part of the DTA curve of the $Y_{20}Ni_{80}$ sample annealed at 600°C.

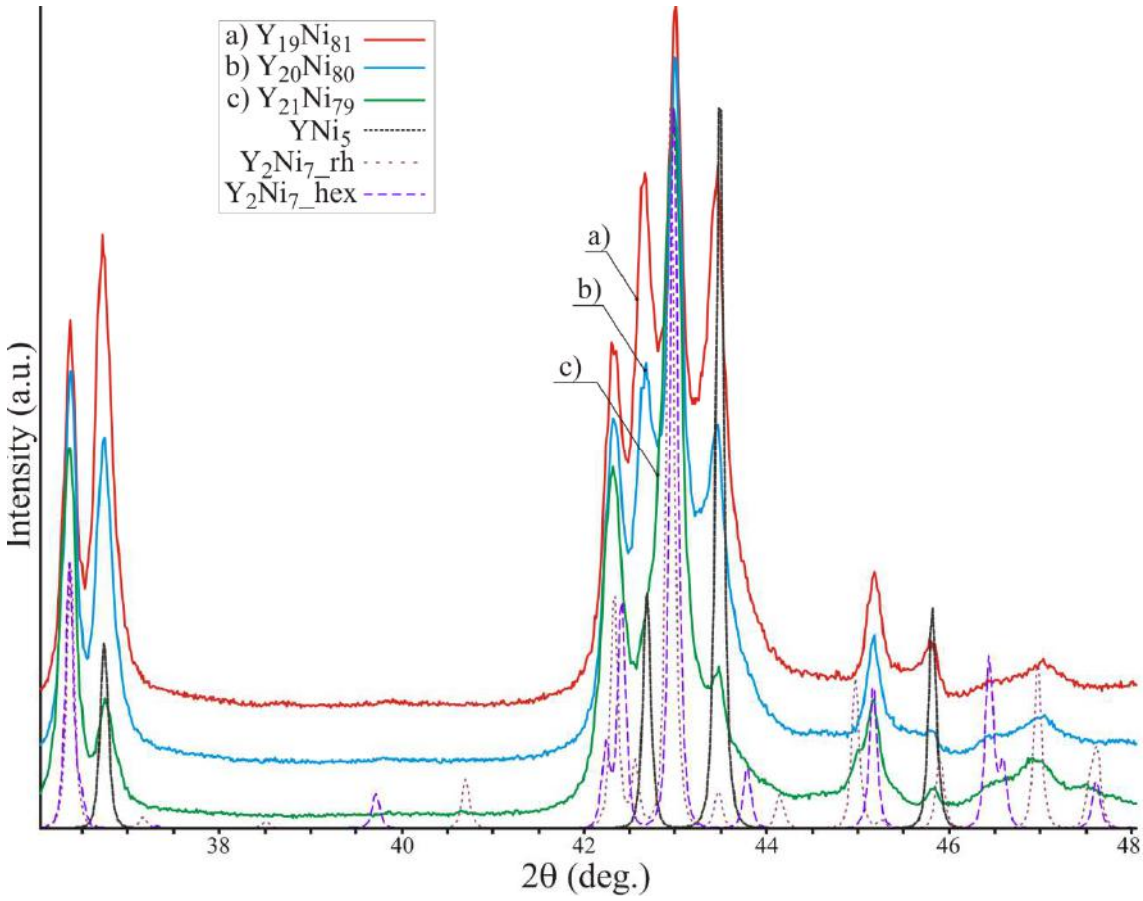

Fig. 6 Experimental XRD profiles of the $Y_{19}Ni_{81}$ (a), $Y_{20}Ni_{80}$ (b), and $Y_{21}Ni_{79}$ (c) alloys annealed at 800°C, theoretical XRD profiles of YNi_5 (black dotted line; $CaCu_5$-type structure), β-Y_2Ni_7 (brown dotted line; rhombohedral β-Gd_2Co_7-type structure), and α-Y_2Ni_7 (lilac dashed line; hexagonal Ce_2Ni_7-type structure).

Table 3 Thermal effects observed by DTA and their interpretation.

Temperature, °C	Reaction	Transformation type
1338±2	$YNi_5 + L \leftrightarrow$ ~YNi_4	Peritectic
1328±2	~$YNi_4 \leftrightarrow L + YNi_5$	Metatectic
1290±2	$YNi_5 + L \leftrightarrow \beta$-$Y_2Ni_7$	Peritectic

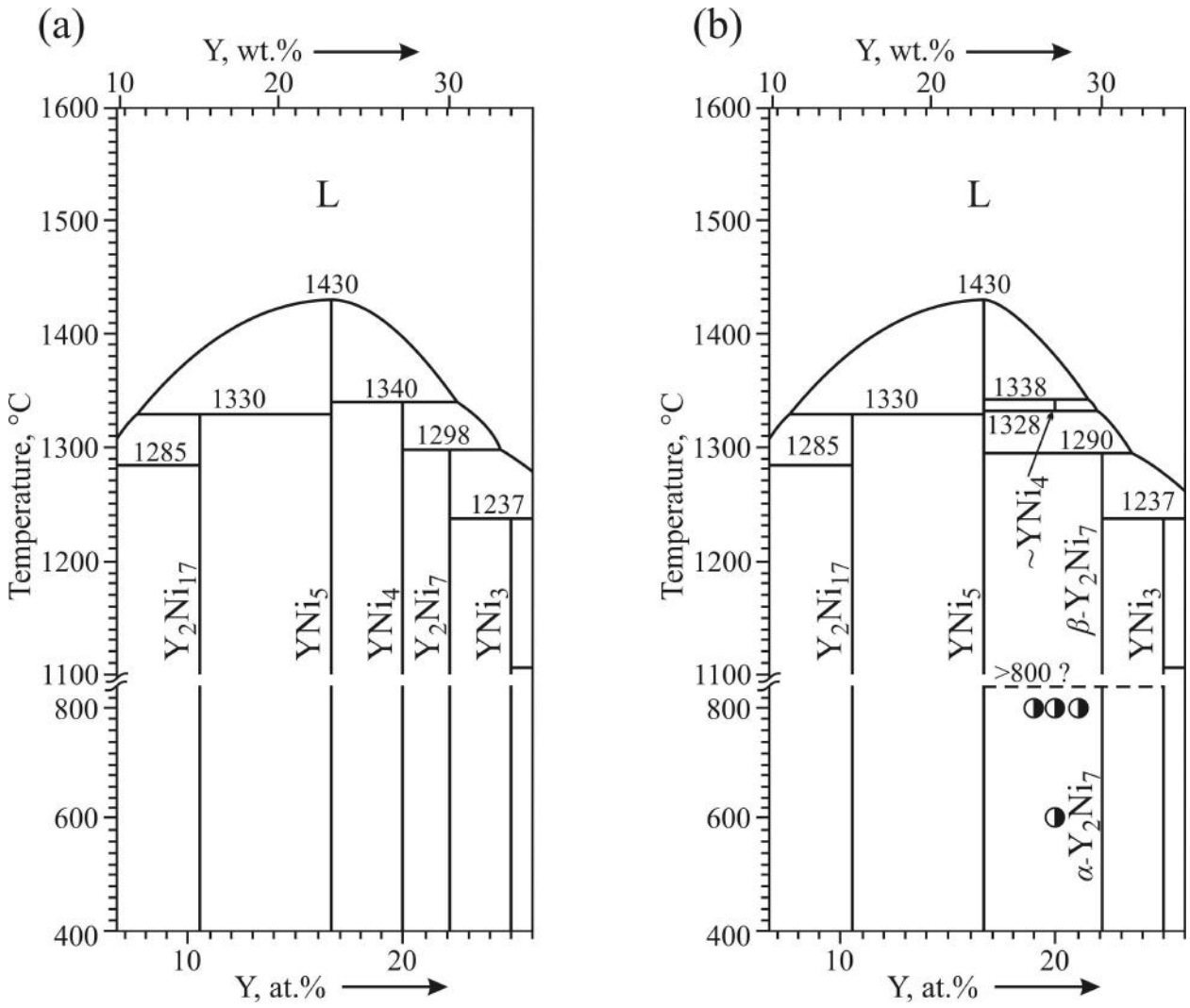

Fig. 7 Phase diagram of the Y–Ni system in the Ni-rich part: based on literature data [4] (a), and updated according to the present study (b).

The results of our study confirm the conclusions of [12] that for the late rare earths with smaller atomic radii, the rhombohedral form (β-Gd_2Co_7 type) is preferred with respect to the hexagonal form (Ce_2Ni_7 type). The latter form is preferred for the early rare earths with larger atomic radii. For rare-earth metals with intermediate radii, including Y, both forms coexist in proportions that depend on the atomic radius. Increasing the annealing temperature and time, in the case of the alloys investigated here, did not allow separating the α- and β-forms of Y_2Ni_7, but led to a change of their ratio. Again, our results are in good agreement with Buschow and van der Goot [12], who state that for compounds with rare-earth atoms with medium-size radii, including Y, the two forms are likely to coexist. The phase transformation proceeds sluggishly and none of two R_2Ni_7 forms can be obtained pure. This may be the reason why we did not observe any thermal effect below 1270°C on the HDSC curve of the $Y_{20}Ni_{80}$ sample. It is also in agreement with the conclusions of [8] concerning the transformation β-Gd_2Ni_7 ↔ α-Gd_2Ni_7.

Based on the present observations we revised the generally accepted Y–Ni phase diagram in the region YNi_5–Y_2Ni_7 [1,2,4], as shown in Fig. 7. Beaudry and Daane [1] concluded that the compound YNi_4 exists

from room temperature up to 1340°C. The revised data show that the ~YNi_4 phase only occurs in a very narrow high-temperature range from 1328±2°C to 1338±2°C. The existence of an intermetallic compound at a composition between RNi_5 and R_2Ni_7, stable in a narrow high-temperatures range, was also observed in the La–Ni system [24]. The two forms of Y_2Ni_7 are indicated in Fig. 7, however, the transformation temperature is only approximate (> 800°C) and needs additional studies to be further specified.

Conclusions

1. The temperature interval of existence of the ~YNi_4 compound was determined. ~YNi_4 forms by the peritectic reaction $YNi_5 + L \leftrightarrow$ ~YNi_4 at 1338±2°C and decomposes by the metatectic reaction ~$YNi_4 \leftrightarrow L + YNi_5$ at 1328±2°C.

2. The samples in the region YNi_5–Y_2Ni_7 annealed for one month at 600°C consisted of two phases: the rhombohedral form β-Y_2Ni_7 (structure type β-Gd_2Co_7, space group *R*-3*m*) and the hexagonal YNi_5 phase (structure type $CaCu_5$, space group *P*6/*mmm*). Annealing at a higher temperature (800°C) for a longer time (five months) caused partial transformation to the low-temperature hexagonal α-Y_2Ni_7 form (structure type Ce_2Ni_7 type, space group $P6_3/mmc$) in a yield of ~23 %. The β-$Y_2Ni_7 \leftrightarrow$ α-Y_2Ni_7 transformation is very sluggish and the alloys in the region YNi_5–Y_2Ni_7 remain in non-equilibrium. The transformation temperature is above 800°C, but additional studies are needed to determine it more precisely.

3. The part of the Y–Ni phase diagram in the range YNi_5–Y_2Ni_7 has been revised.

References

[1] B.J. Beaudry, A.H. Daane, *Trans. Met. Soc. AIME* 218 (1960) 854-859.

[2] R.F. Domagala, J.J. Rausch, D.W. Levinson, *Trans. ASM* 53 (1961) 137-155.

[3] K.H.J. Buschow, *J. Less-Common Met.* 11 (1966) 204-208.

[4] P. Nash (Ed.), *Binary Alloy Phase Diagrams*, ASM International, Materials Park, OH, 1991, p. 2885.

[5] P.R. Subramanian, J.F. Smith, *Metall. Trans. B* 16 (1985) 577-584.

[6] Z. Du, W. Zhang, *J. Alloys Compd*. 245 (1996) 164-167.

[7] R. Lemaire, D. Paccard, R. Pauthenet, *C. R. Acad. Sci., Ser. B* 265 (1967) 1280-1282.

[8] A.V. Virckar A. Raman, *J. Less-Common Met.* 18 (1969) 59-66.

[9] D.T. Cromer, A.C. Larson, *Acta Crystallogr*. 12 (1959) 855-859.

[10] E.F. Bertaut, R. Lemaire, J. Schweizer, *Bull. Soc. Fr. Mineral. Cristallogr.* 88 (1965) 580-585.

[11] A.E. Dwight, *Trans. Am. Soc. Met.* 53 (1961) 479-500.

[12] K.H.J. Buschow, A.S. van der Goot, *J. Less-Common Met.* 22 (1970) 419-428.

[13] C. Colinet, A. Pasturel, K.H.J. Buschow, *J. Appl. Phys.* 62 (1987) 3712-3717.

[14] O. Myakush, V. Babizhetskyy, V. Levytskyy, B. Kotur, *Chem. Met. Alloys* 9 (2016) 1-10.

[15] E. Parthé, B.A. Chabot, K. Cenzual, *Chimia* 39 (1985) 164-174.

[16] M. Mezbahul-Islam, M. Medraj, *Mater. Sci. Techn.*, Pittsburgh, USA, 2008, Vol. 2, p. 1017-1028.

[17] W. He, W. Zheng, J. Yang, L. Zeng, *J. Alloys Compd.* 509 (2011) 6794-6799.

[18] S. Pan, H Zhou, Q. Zhou, Q. Yao, Z. Wang, *J. Alloys Compd*. 471 (2009) 119-121.

[19] M. Mezbahul-Islam, M. Medraj, *J. Solid State Chem.* 561 (2013) 161-173.

[20] V. Babizhetskyy, O. Myakush, B. Kotur, A. Simon, *Intermetallics* 38 (2013) 44-48.

[21] L. Akselrud, Yu. Grin, *J. Appl. Crystallogr.* 47 (2014) 803-805.

[22] V. Levytskyy, V. Babizhetskyy, B. Kotur, V. Smetana, *Acta Crystallogr. E* 68 (2012) i20.

[23] V. Levytskyy, V. Babizhetskyy, B. Kotur, *Visn. Lviv. Univ., Ser. Khim.* 55 (2014) 12-20.

[24] H. Inui, T. Yamamoto, Z. Di, M. Yamaguchi, *J. Alloys Compd*. 293-295 (1999) 140-145.